CORRESPONDENCE

Reply to "Comments on 'A *CloudSat–CALIPSO* View of Cloud and Precipitation Properties across Cold Fronts over the Global Oceans'"

CATHERINE M. NAUD

Department of Applied Physics and Applied Mathematics, Columbia University, and NASA Goddard Institute for Space Studies, New York City, New York

DEREK J. POSSELT

Jet Propulsion Laboratory, California Institute of Technology, Pasadena, California

SUSAN C. VAN DEN HEEVER

Department of Atmospheric Science, Colorado State University, Fort Collins, Colorado

(Manuscript received 14 November 2017, in final form 31 January 2018)

ABSTRACT

In Naud et al., a compositing method was utilized with *CloudSat–CALIPSO* observations to obtain mean transects of cloud vertical distribution and surface precipitation across cold fronts, and to examine their sensitivity to the large-scale properties of the parent extratropical cyclone. This reply demonstrates the value of compositing for evaluating numerical models, and presents additional results that address the issue of the sensitivity of the initial results to the frontal detection methodology and the potential misclassification of occlusions as cold fronts. Here a sensitivity study of the cold front composite transects of cloud cover to the input datasets or the method utilized to locate the cold fronts demonstrates that these composite transects are robust and only marginally sensitive to cold front location methods. The same conclusion is reached for the robustness of the contrast between Northern and Southern Hemisphere cloud transects. While occlusions cannot directly be flagged within the database at this point, comparisons of transects obtained for subsets of cyclones of different age indicate that the misclassification of occluded fronts as cold fronts does not explain the predominance of cloud and precipitation on the warm side of the cold fronts. The strong signal on the warm side might be better explained by a predominance of forward sloping cold fronts, or the presence of the warm conveyor belt.

1. On the compositing method

Compositing has proven utility for climatological studies. One of the primary uses of observational composites is in the evaluation or constraint of numerical models. While composites highlight the most salient features of a system, they also integrate all of the variability across multiple systems. In addition, compositing helps to extract valuable information from datasets that are spatially and/or temporally sparse. Use of satellite data composites for the examination of the cloud type spatial distribution of extratropical cyclones (ETCs) was pioneered by Lau and Crane (1995). Their composited observations were then used to evaluate cloud representation in a reanalysis (Klein and Jakob 1999). Cyclone-centered compositing of satellite observations has since been used extensively since for both model evaluation and cyclone specific studies; we cannot cite all of these studies, but provide a few key examples here. Bauer and Del Genio (2006) used compositing to explore moisture distribution in the midlatitudes in a general circulation model (GCM); Field and Wood (2007) explored the relationship between precipitation, cyclone strength, and environmental moisture amount in the warm conveyor belt region of the cyclones, and subsequently to evaluate the impact of different parameterizations in a GCM (Field et al. 2008); and

Corresponding author: Catherine Naud, catherine.naud@columbia.edu

DOI: 10.1175/JCLI-D-17-0777.1

Govekar et al. (2011) explored the three-dimensional structure of clouds and ultimately used the relation between this structure and large-scale conditions to evaluate a GCM (Govekar et al. 2014). These studies used the center of the extratropical cyclones as an anchor to construct the cyclone-centered composite mean. However, it has become apparent that delineating frontal structures could provide more detail on the structure and characteristics of midlatitude systems. For example, Berry et al. (2011) created a database and climatology of frontal boundaries, which was subsequently used by Catto et al. (2012) to derive frontal contributions to the total midlatitude precipitation. Naud et al. (2010) used cloud observations from *CloudSat–CALIPSO* (Mace and Zhang 2014) to evaluate a GCM's ability to represent the vertical distribution of cloud across warm and cold fronts and its sensitivity to the large-scale properties of the cyclones.

The Naud et al. (2015) study makes use of a well-established technique to explore cloud and precipitation distribution in cold frontal regions on a global scale, along with their sensitivity to the larger-scale environment. As such, it is a climatological study that uses a compositing method to integrate over a large number of individual cold fronts for the purpose of obtaining the most common frontal features. Because of *CloudSat*'s narrow swath (~1.5 km; Stephens et al. 2002), this method also compensates for nonuniform and sparse information to obtain vertical profiles of cloud occurrence using multiple events. In this manner, the study achieves our stated scientific goal which is to "better understand the link between environmental conditions and the amount of clouds and precipitation across cold fronts" (cf. Naud et al. 2015, third paragraph of the introduction).

If the variability is large across individual cases, the resulting composite might not match (and in fact is likely not to match) the classic picture of cold frontal structure (Bjerknes 1919). For example, information on the direction of cloud slope with height might be lost because the slopes might not be collocated across all cold fronts. Similarly, rainbands may not be collocated with respect to the cold front location from one case to another. Consequently, in the composite mean, these features will be blurred and thus less clearly defined than in each individual case. This approach does, however, cause the strongest signal (e.g., from the clouds and precipitation in the warm conveyor belt; Browning 1986) to stand out in the average. If one is primarily interested in the total cloud cover (which is one of the two aspects of clouds that matter most for the radiative impact in climatology), the overall amount of precipitation associated with these systems, and the sensitivity of these two fields to changes in large-scale conditions, then compositing in this manner is a very useful tool. Perhaps more importantly, while construction of a grand unified mean state is useful, the most powerful aspect of compositing lies in the collection of a large diversity of samples for analysis.

2. On the sensitivity of the composites to the cold front detection method

In Naud et al. (2015), two separate methods were used to locate cold fronts in extratropical cyclones. One was proposed by Hewson (1998) and based on temperature gradients, the other by Simmonds et al. (2012) and based on wind direction changes. According to Schemm et al. (2015), the two methods are complementary: the Hewson (1998) method performs best in systems with high baroclinicity, whereas the Simmonds et al. (2012) method performs best in systems with low baroclinicity (their first bullet point in their conclusions section). As such, by using both methods, we ensure that we include a full range of system types in the database. This enhances, rather than degrades, the quality of the composites. In addition, because we are interested in sensitivities (and thus examining differences between composites), the most important consideration is that the method used to detect the fronts be the same for different seasons, hemispheres, and environmental conditions. A comprehensive description of the combined method is provided in Naud et al. (2016); to avoid repetition, we refer readers interested in applying a similar method to that paper. In addition, the database of cold and warm front detections used here is now public and available online (see acknowledgments).

To provide a more qualitative view of the impact of the front detection method on the cloud transect composites, we show a new version of Fig. 1 of Naud et al. (2015), now obtained using MERRA-2 (Gelaro et al. 2017) for the front detections [instead of MERRA as in Naud et al. (2015)], and the latest version of the *CloudSat* cloud product [release R05 vs R04 in Naud et al. (2015)]. The reason behind the use of different input datasets is to demonstrate the robustness of the composites. Figure 1 shows the cloud composite transects for all maritime cold frontal regions (i.e., both hemispheres) when using the combined cold front detection method described in Naud et al. (2016) as anchor (Fig. 1b), as well as composites obtained separately, using either the Hewson (1998) detections (Fig. 1c) or the Simmonds et al. (2012) detections (Fig. 1d). For reference, the original composite from Naud et al. (2015) is also shown (Fig. 1a). We expect the composites to differ between the three different methods because of the differing characteristics of the cyclones that are sampled by each. And indeed, there are small differences

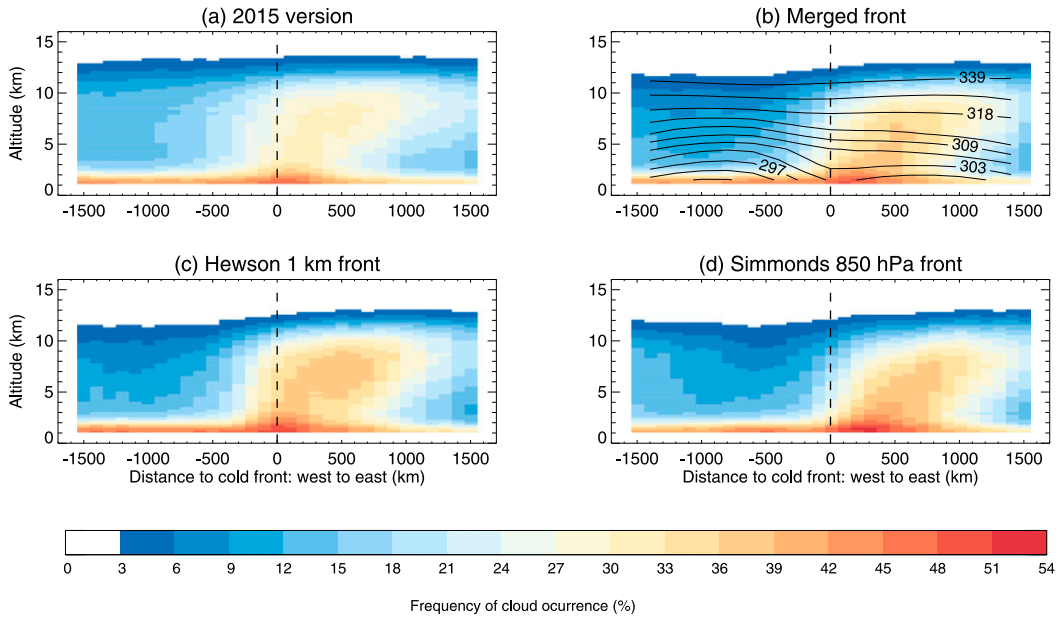

FIG. 1. Frequency of cloud occurrence across cold fronts in the midlatitudes (30°–60°N/S) from November 2006 to October 2010 obtained with (a) MERRA and R04 *CloudSat–CALIPSO* cloud retrieval as in Fig. 1 of Naud et al. (2015) and (b)–(d) MERRA2 and R05 *CloudSat-CALIPSO* retrievals. The vertical dashed line indicates the location of the surface front obtained with the combined method of Naud et al. (2015), the method of Naud et al. (2016), the Hewson (1998) method, and the Simmonds et al. (2012) method in (a)–(d), respectively. The solid contours in (b) represent the mean composite of MERRA-2 equivalent potential temperature.

between these figures (Figs. 1b–d) and Fig. 1a (the 2015 composite), but qualitatively the cloud distribution is very similar, suggesting that our composites are robust.

More importantly, as we are interested in sensitivities, we also examine how the composite differences between NH and SH clouds change when using different front detection methods (Fig. 2). Again, as anticipated, the composite differences (Figs. 2b–d) are not exactly the same as those in Naud et al. (2015) (Fig. 2a). The NH versus SH differences above 8 km are weaker than in Naud et al. (2015) on the cold side of the front, while the differences below 2 km are stronger. There are also slight differences between Figs. 2b, 2c, and 2d, but overall the conclusions we made in Naud et al. (2015) are still valid, regardless of the version of the input data and the cold front detection method we use. Differences between the NH and SH can only be explained if, in addition to the differences in precipitable water (PW) and ascent strength between the two hemispheres, we also take into account the impact on the NH–SH differences of the temperature contrast across fronts.

3. On the possible misclassification of occluded fronts

Inclusion of occluded fronts in our warm and cold front database is potentially a problem, and stems from the fact that, to our knowledge, there is no simple objective test that can be applied to determine whether a front is occluded. In Hewson (1998), geostrophic temperature advection is used to delineate warm and cold fronts, and he acknowledges: "the new techniques described in this paper will generally not omit occluded fronts, but instead plot them as either a cold front, or a warm front, or a near-parallel cold front/warm front pair" (p. 52).

The test proposed by Hewson (1998), and used in our front identification routine, involves calculation of the geostrophic thermal advection ($A_{G\tau}$); that is, $A_{G\tau} = -\mathbf{V}_G \cdot \nabla\tau$ for each frontal point (where $\mathbf{V}_G$ is the geostrophic wind and τ the thermal parameter, here the potential temperature). If the geostrophic wind advects the frontal point toward warmer temperature, then $A_{G\tau} < 0$, and the frontal point is considered to be a cold frontal point. If the geostrophic wind advects the point toward cold temperature, then $A_{G\tau} > 0$ and the frontal point is considered to be a warm frontal point.

According to Schultz and Mass (1993), Schultz and Vaughan (2011), or Schultz et al. (2014), the most common occlusion type is the warm type. In some cases, this means that the temperature in advance of the front is lower than the temperature in the wake of the front. In this case, the test proposed by Hewson (1998) will preferentially flag an occlusion as a warm front rather

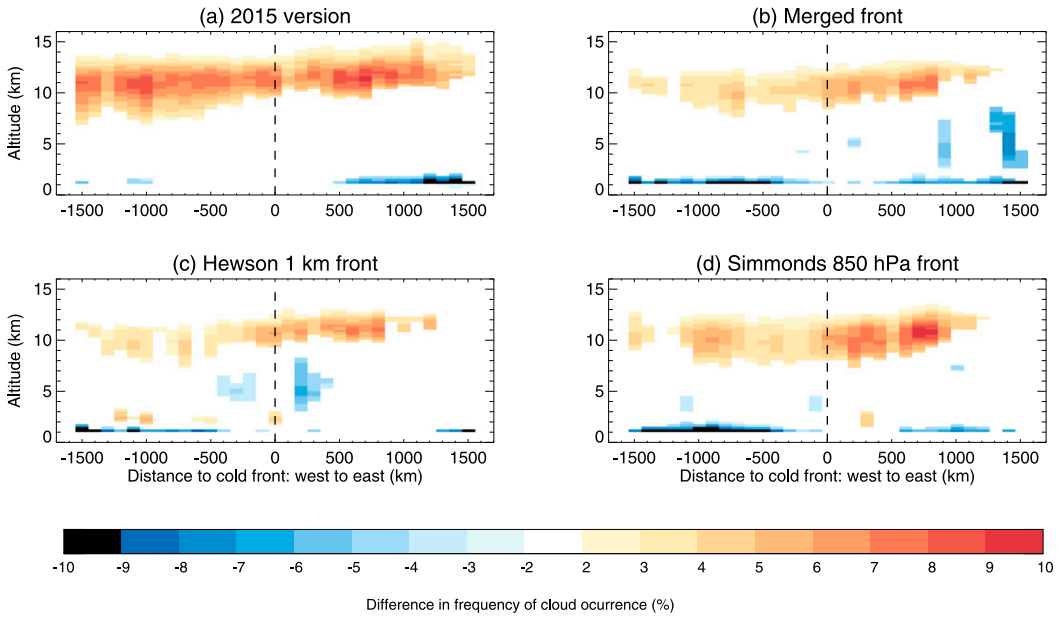

FIG. 2. Difference in frequency of cloud occurrence between NH and SH cold fronts for all seasons. (a) Shown here is Fig. 13 of Naud et al. (2015). (b)–(d) The vertical dashed lines indicate the location of the surface front obtained with the combined method of Naud et al. (2016), the Hewson (1998) method, and the Simmonds et al. (2012) method, respectively. As in Naud et al. (2015), differences are only shown when larger than one standard deviation as presented in Fig. 2 of Naud et al. (2015).

than a cold front. However, as Stoelinga et al. (2002) reported, this temperature contrast is not always the sign of the warm-type occlusion, and so this front typing flag does not, in and of itself, ensure that there are no occluded fronts in the cold front database. Nevertheless, we addressed this issue in the Naud et al. (2015) study when assigning a *CloudSat–CALIPSO* profile to a given cold frontal region: profiles found within a 500-km radius region surrounding the cyclone low pressure center are not included in the cloud and precipitation cold-front centered composites.

If we could isolate storms for which we are sure that the occlusion has not occurred, we could verify whether the associated cloud transect composite looks any different from the mean over all systems. This would at least give us some indication of the potential for occluded fronts to be misclassified as cold fronts in our database. In an attempt to mimic this, we subset our cold front database to retain only those cases for which the cold front is strictly located to the west of the low pressure center. This criterion is a first-order condition, which ensures that, as illustrated by Figs. 2i and 12i in Schultz and Vaughan (2011), these cold fronts are mostly confined to systems that are unlikely to be occluded. We then construct a second subset that includes only cold fronts found to the east of the low pressure center. These cold fronts are considered to be included in systems that may be undergoing occlusion. For each subset, we construct the cloud frequency of occurrence composite transects and look at the difference between the two subsets (i.e., western vs eastern fronts). If a portion of the cold fronts we identify in the second set are, in fact, warm-type occluded fronts, then the two composites should look different. As stated in Schultz (2018), occluded fronts exhibit a forward sloping cloud pattern (e.g., Fig. 10a in Posselt et al. 2008), while a classic cold front exhibits a rearward-sloping cloud pattern (e.g., Fig. 4a in Posselt et al. 2008). As such, the differences between the two subset composites defined above should indicate cloud cover at all altitudes that is much larger in the second (possibly occluded) than in the first (not occluded) set on the eastern side of the composites. Figure 3 shows the difference in frequency of cloud occurrence composites between the occlusion-free and possibly contaminated subsets. The difference is noisy but suggests slightly less cloud at midtropospheric levels eastward of the front in the occlusion-free subset. However, with differences in the 5%–7% range, this figure does not indicate any clear evidence of contamination by occlusion.

We perform an additional test by using the storm tracks to estimate the age of the cyclone for each of the cold front detections in our *CloudSat–CALIPSO* dataset. Our rationale is that the likelihood that a system will

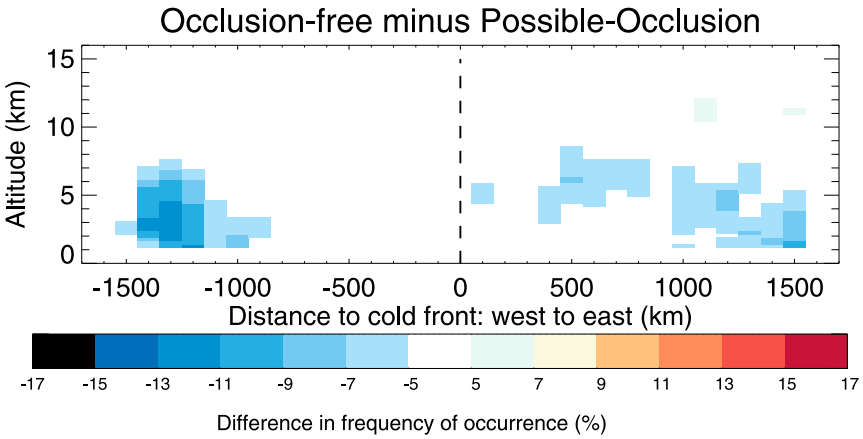

FIG. 3. Difference in frequency of cloud occurrence across cold fronts between cold fronts confined to the west of the low-pressure center and cold fronts confined to the east.

be occluded in the first part of its evolution is small. To measure the age of the cyclones, we estimate the time of peak intensity as the time of maximum depth (Rudeva and Gulev 2011; Polly and Rossow 2016): peak intensity is reached when the difference in pressure between the outermost closed pressure contour and the center of the cyclone is at a maximum. Once we have identified the time of peak intensity, we divide the time period between first detection and peak intensity into two equal periods, and consider the first one to be the onset or development phase. As stated above, the onset period is likely to have a much smaller incidence of occlusions. As before, we construct the cloud cover composite transect for the onset cold front subset (Fig. 4). This figure shows that the subset with the least probability of being contaminated by occluded fronts shows a much larger amount of clouds at all levels in the warm sector than the full set (Fig. 1), and still indicates no rearward slope in the cloud fraction. Moreover, the composite mean of MERRA-2 equivalent potential temperature overlaid in Fig. 1b suggests that on average the cold fronts in the database are rearward sloping. While we cannot entirely rule out misclassification of occluded fronts as cold fronts, we can conclude that any inclusion of occluded fronts in the database has little effect on the composite mean spatial distribution of clouds across cold fronts. The fact that the signal is largest in the warm sector, rather than the cold sector, again also demonstrates that composites are not similar to individual cases, and that the most salient feature dominates the signal regardless of the specific characteristics of the cold fronts themselves. Here, we hypothesize that this relative maximum in cloud cover on the warm side of the surface cold front might be strongly influenced by the presence of warm conveyor belts, while we acknowledge that even though most warm conveyor belts are found in the warm sector

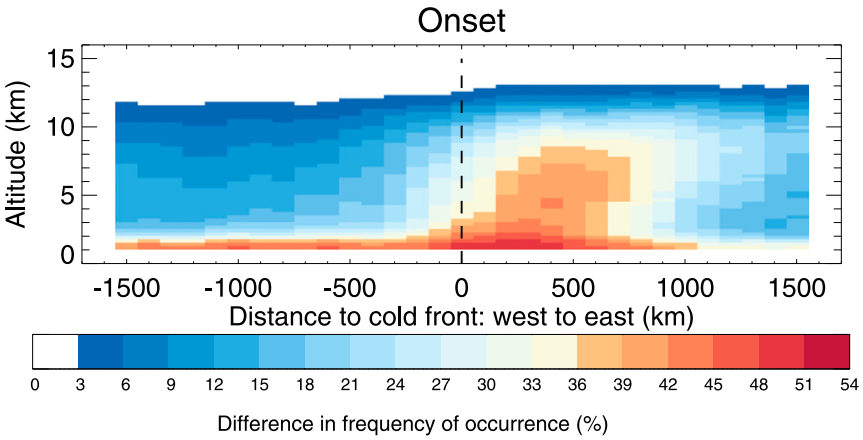

FIG. 4. As in Fig. 1b, but for cold fronts located in cyclones in the first stage of their evolution, from first detection to half the time to peak intensity.

of a cyclone, not all cyclones include a warm conveyor belt within 1000 km of the center (Eckhardt et al. 2004).

4. Conclusions

In this reply, we address the concerns of Schultz (2018), which are 1) the inclusion of occluded fronts in the composites of cold fronts, 2) the inclusion of multiple different types of cold fronts in the composites, 3) the use of two different approaches to locate cold fronts, and 4) the fact that compositing over a large number of fronts obscures alongfront variability. To address the first point, we present results from a series of tests that demonstrate that contamination by occluded fronts is not responsible for the overall distribution of clouds across the cold front composites. To address the second point, we argue that composites should ideally include as much variability as possible to give an accurate mean representation of cloud and precipitation across cold fronts. The third point is addressed by presenting additional tests to demonstrate that the cold front location method has little impact on the overall mean distribution of clouds across cold fronts. Finally, the fourth point concerns the alongfront variability, which is inherently not taken into account in the transect composites. The investigation of along- or cross-front variability cannot be adequately performed using a compositing technique and would be better conducted with a series of case studies. Such an analysis would necessarily be the subject of an entirely different and separate study.

The goals of the Naud et al. (2015) study were 1) to integrate over as many types of cold front structure as possible, in numbers that are as near as possible to what occurs in the real world, and 2) to examine the overall cloud cover (and precipitation distribution), and its sensitivity to various large-scale environmental conditions. As such, we disagree with the conclusions of Schultz (2018) as one can *only* generalize about cold fronts in the aggregate by including an unspecified number of diverse frontal structures and characteristics. In a climatological framework, and for model evaluation (especially for climate models, which cannot be expected to reproduce specific fronts), our study is entirely appropriate. For more specific analyses of the frontal mesoscale structure and the dynamical evolution of fronts themselves, we agree that a more fine-grained analysis would be required. Finally, we have made our frontal database public specifically so that such further analyses may be conducted, and we welcome partnership in this effort.

Acknowledgments. The work was funded by NASA CloudSat Science Team Recompete Grant NNX13AQ33G. The database of cold and warm fronts associated with extratropical cyclones is stored at the NASA Center for Climate Simulation data portal and available through https://data.giss.nasa.gov/storms/obs-etc. We are grateful to two anonymous reviewers and Steve Klein for their helpful comments.

REFERENCES

Bauer, M., and A. D. Del Genio, 2006: Composite analysis of winter cyclones in a GCM: Influence on climatological humidity. *J. Climate*, **19**, 1652–1672, https://doi.org/10.1175/JCLI3690.1.

Berry, G., C. Jakob, and M. Reeder, 2011: Recent global trends in atmospheric fronts. *Geophys. Res. Lett.*, **38**, L21812, https://doi.org/10.1029/2011GL049481.

Bjerknes, J., 1919: On the structure of moving cyclones. *Mon. Wea. Rev.*, **47**, 95–99, https://doi.org/10.1175/1520-0493(1919)47<95:OTSOMC>2.0.CO;2.

Browning, K. A., 1986: Conceptual models of precipitation systems. *Wea. Forecasting*, **1**, 23–41, https://doi.org/10.1175/1520-0434(1986)001<0023:CMOPS>2.0.CO;2.

Catto, J. L., C. Jakob, G. Berry, and N. Nicholls, 2012: Relating global precipitation to atmospheric fronts. *Geophys. Res. Lett.*, **39**, L10805, https://doi.org/10.1029/2012GL051736.

Eckhardt, S., A. Stohl, H. Wernli, P. James, C. Forster, and N. Spichtinger, 2004: A 15-year climatology of warm conveyor belts. *J. Climate*, **17**, 218–237, https://doi.org/10.1175/1520-0442(2004)017<0218:AYCOWC>2.0.CO;2.

Field, P. R., and R. Wood, 2007: Precipitation and cloud structure in midlatitude cyclones. *J. Climate*, **20**, 233–254, https://doi.org/10.1175/JCLI3998.1.

——, A. Gettelman, R. B. Neale, R. Wood, P. J. Rasch, and H. Morrison, 2008: Midlatitude cyclone compositing to constrain climate model behavior using satellite observations. *J. Climate*, **21**, 5887–5903, https://doi.org/10.1175/2008JCLI2235.1.

Gelaro, R., and Coauthors, 2017: The Modern-Era Retrospective Analysis for Research and Applications, version 2 (MERRA-2). *J. Climate*, **30**, 5419–5454, https://doi.org/10.1175/JCLI-D-16-0758.1.

Govekar, P. D., C. Jakob, M. J. Reeder, and J. Haynes, 2011: The three-dimensional distribution of clouds around Southern Hemisphere extratropical cyclones. *Geophys. Res. Lett.*, **38**, L21805, https://doi.org/10.1029/2011GL049091.

——, ——, and J. Catto, 2014: The relationship between clouds and dynamics in Southern Hemisphere extratropical cyclones in the real world and a climate model. *J. Geophys. Res. Atmos.*, **119**, 6609–6628, https://doi.org/10.1002/2013JD020699.

Hewson, T. D., 1998: Objective fronts. *Meteor. Appl.*, **5**, 37–65, https://doi.org/10.1017/S1350482798000553.

Klein, S. A., and C. Jakob, 1999: Validation and sensitivities of frontal clouds simulated by the ECMWF model. *Mon. Wea. Rev.*, **127**, 2514–2531, https://doi.org/10.1175/1520-0493(1999)127<2514:VASOFC>2.0.CO;2.

Lau, N.-C., and M. W. Crane, 1995: A satellite view of the synoptic-scale organization of cloud properties in midlatitude and tropical circulation systems. *Mon. Wea. Rev.*, **123**, 1984–2006, https://doi.org/10.1175/1520-0493(1995)123<1984:ASVOTS>2.0.CO;2.

Mace, G. G., and Q. Zhang, 2014: The *CloudSat* radar–lidar geometrical profile product (RL-GeoProf): Updates, improvements,

and selected results. *J. Geophys. Res. Atmos.*, **119**, 9441–9462, doi:10.1002/2013JD021374.

Naud, C. M., A. D. Del Genio, M. Bauer, and W. Kovari, 2010: Cloud vertical distribution across warm and cold fronts in *CloudSat–CALIPSO* data and a general circulation model. *J. Climate*, **23**, 3397–3415, https://doi.org/10.1175/2010JCLI3282.1.

——, D. J. Posselt, and S. C. van den Heever, 2015: A *CloudSat–CALIPSO* view of cloud and precipitation properties across cold fronts over the global oceans. *J. Climate*, **28**, 6743–6762, https://doi.org/10.1175/JCLI-D-15-0052.1.

——, J. F. Booth, and A. D. Del Genio, 2016: The relationship between boundary layer stability and cloud cover in the post-cold-frontal region. *J. Climate*, **29**, 8129–8149, https://doi.org/10.1175/JCLI-D-15-0700.1.

Polly, J. B., and W. B. Rossow, 2016: Cloud radiative effects and precipitation in extratropical cyclones. *J. Climate*, **29**, 6483–6507, https://doi.org/10.1175/JCLI-D-15-0857.1.

Posselt, D. J., G. L. Stephens, and M. Miller, 2008: CloudSat: Adding a new dimension to a classical view of extratropical cyclones. *Bull. Amer. Meteor. Soc.*, **89**, 599–609, https://doi.org/10.1175/BAMS-89-5-599.

Rudeva, I., and S. K. Gulev, 2011: Composite analysis of North Atlantic extratropical cyclones in NCEP–NCAR reanalysis data. *Mon. Wea. Rev.*, **139**, 1419–1446, https://doi.org/10.1175/2010MWR3294.1.

Schemm, S., I. Rudeva, and I. Simmonds, 2015: Extratropical fronts in the lower troposphere—Global perspectives obtained from two automated methods. *Quart. J. Roy. Meteor. Soc.*, **141**, 1686–1698, https://doi.org/10.1002/qj.2471.

Schultz, D. M., 2018: Comments on "A *CloudSat–CALIPSO* view of cloud and precipitation properties across cold fronts over the global oceans." *J. Climate*, **31**, 2965–2967, https://doi.org/10.1175/JCLI-D-17-0619.1.

——, and C. F. Mass, 1993: The occlusion process in a midlatitude cyclone over land. *Mon. Wea. Rev.*, **121**, 918–940, https://doi.org/10.1175/1520-0493(1993)121<0918:TOPIAM>2.0.CO;2.

——, and G. Vaughan, 2011: Occluded fronts and the occlusion process: A fresh look at conventional wisdom. *Bull. Amer. Meteor. Soc.*, **92**, 443–466, https://doi.org/10.1175/2010BAMS3057.1.

——, B. Antonescu, and A. Chiariello, 2014: Searching for the elusive cold-type occluded front. *Mon. Wea. Rev.*, **142**, 2565–2570, https://doi.org/10.1175/MWR-D-14-00003.1.

Simmonds, I., K. Keay, and J. A. T. Bye, 2012: Identification and climatology of Southern Hemisphere mobile fronts in a modern reanalysis. *J. Climate*, **25**, 1945–1962, https://doi.org/10.1175/JCLI-D-11-00100.1.

Stephens, G. L., and Coauthors, 2002: The *CloudSat* mission and the A-TRAIN: A new dimension to space-based observations of clouds and precipitation. *Bull. Amer. Meteor. Soc.*, **83**, 1771–1790, https://doi.org/10.1175/BAMS-83-12-1771.

Stoelinga, M. T., J. D. Locatelli, and P. V. Hobbs, 2002: Warm occlusions, cold occlusions, and forward-tilting cold fronts. *Bull. Amer. Meteor. Soc.*, **83**, 709–721, https://doi.org/10.1175/1520-0477(2002)083<0709:WOCOAF>2.3.CO;2.